OPTICAL DESIGN OF THE PI-TEST MEBT BEAM SCRAPING SYSTEM*

A. Saini†, A. Shemyakin, Fermi National Accelerator Laboratory, Batavia, USA

Abstract

PI-Test [1] is an accelerator facility under construction at Fermilab that will provide a platform to demonstrate critical technologies and concept of front-end of the PIP-II superconducting radio frequency (SRF) linac. It will be capable to accelerate an H^- ion beam with average current of 2 mA up to 25 MeV in continuous wave (CW) regime. To protect the SRF components from beam irradiation, the Medium Energy Beam Transport (MEBT) section of PI-Test includes an elaborated beam scraping system. It consists of four assemblies spread along the MEBT, with each assembly composed of four radiation-cooled, electrically isolated plates that can be moved into the beam in horizontal and vertical direction. The primary objectives of scraping system are to intercept particles with large transverse action and to protect the beamline elements and SRF linac in case of errors with beam focusing or steering. In this paper we formulate requirements for the scraping system and discuss factors affecting its efficiency. An optical design compatible with PI-Test MEBT is also presented.

INTRODUCTION

The uncontrolled beam loss in a linac may result in beam interruptions, radio-activation, and hazard to environment. As discussed elsewhere [2], continuous beam loss on the surface of SRF cavity causes a degradation in its performance. One of the means to decrease the beam loss in the SRF accelerating section of a linac is to install a scraping system at its low energy normal conducting section. Scrapers installed at optimum locations limit the phase space of particles that can enter the SRF and therefore, it allows not only to remove halo particles but also to intercept the beam core in case of errors with focusing or steering of the beam. In this paper we first discuss formulation of the efficiency of a scraping system and then present a realization of the concept at the PI-Test MEBT.

FORMALISM

One-plane (e.g. x) particle motion in the phase space in presence of uncoupled linear fields is characterized by its action (J):

$$J = \frac{1}{2}\left(\gamma x^2 + 2\alpha x x' + \beta x'^2\right); \tag{1}$$

where α, β, γ are Twiss parameters and x, x' are coordinates of the particle. Particles with large actions outline the beam boundary and, in practice, potential beam loss either due to the beam halo formation or focusing errors. A set of two scrapers inserted symmetrically at a particular location remove particles with large spatial offsets but do not limit the maximum action in the beam (Fig. 1). For the latter, second set of scraper needs to be placed downstream to remove particles that had large angles but small offsets at location of the first set. The efficiency of such scraping system is described by the maximum action left after scraping of a fraction ΔN of the particle distribution.

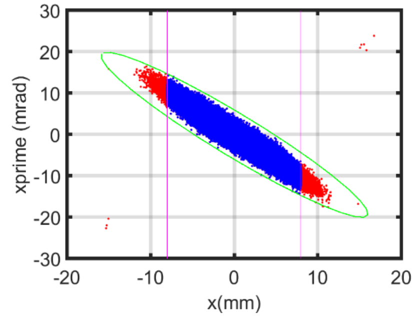

Figure 1: Horizontal beam phase space distribution before (red) and after (blue) a scraper assembly (magenta lines). The particle exhibiting maximum action in the phase space after a beam scraping moves along green ellipse.

Let us consider a beam with an initial Gaussian distribution:

$$g(x,x') = \frac{1}{2\pi\sigma_x\sigma_{x'}} e^{-\left(\frac{(x-\bar{x})^2}{2\sigma_x^2} + \frac{(x'-\bar{x}')^2}{2\sigma_{x'}^2}\right)} = \frac{e^{\frac{-J}{\varepsilon_0}}}{\varepsilon_0}; \tag{2}$$

where ε_0 is the rms emittance and σ_x, $\sigma_{x'}$ are rms beam size and angle respectively. The scraping system is described by edge to edge separation $2d_i$ between two scrapers facing each other in an assembly i and the betatron phase advance $\Delta\phi$ between two successive scraper assemblies. Normalization of the the scraper insertion w.r.t rms beam size is expressed as:

$$a_i = \frac{d_i}{\sqrt{\beta\varepsilon_0}} \tag{3}$$

A fraction N_i of the beam intercepted at each set can be expressed as:

$$N_1(a_1) = 1 - erf(a1);$$

$$N_2(a_1, a_2, \Delta\varphi) = \frac{1}{\sqrt{\pi}} \int_{-a_1}^{a_1} e^{-u^2}\left(1 - erf\left(\frac{a_2 - u\cos(\Delta\varphi)}{\sin(\Delta\varphi)}\right)\right) du \tag{4}$$

Maximum action normalized to rms beam emittance after the second scraper assembly is calculated using following equation:

$$J_{\max} = \frac{a_1^2 + 2a_1 a_2 \left|\cos(\Delta\varphi)\right| + a_2^2}{\sin(\Delta\varphi)^2} \tag{5}$$

If fraction of the beam scraped at each location is limited due to constraints such as scraper design specification, outgassing issues, etc., it is reasonable to consider the case when same portion of beam is scraped at both scraper assemblies that implies $N_1 = N_2 = \Delta N/2$. For known values of ΔN and, $\Delta\phi$ equation (4) can be solved numerically to determine corresponding insertion of scrapers. Then, using equation (5) one can express normalized action as a function of ΔN and, $\Delta\phi$ i.e. $J_{max}(\Delta N, \Delta\phi)$. An estimation has

* Work supported by Fermi Research Alliance, LLC under Contracts No. De-Ac02-07CH11359 with the DOE, USA.
† asaini@fnal.gov

ISBN 978-3-95450-169-4

been performed using a MathCad script to understand dependence of normalized action on ΔN and $\Delta\phi$. Results are shown in Fig. 2 and Fig. 3. The maximum action minimizes at $\Delta\phi = 90^0$ and depends logarithmically on the total fraction of beam scraped out. At $\Delta\phi = 90^0$ and for the interesting range of scraping fraction, maximum normalized action can be approximated as:

$$J_{max}\left(\Delta N, \frac{\pi}{2}\right) \approx -1 - 1.9 * \ln(\Delta N) \quad . \qquad (6)$$

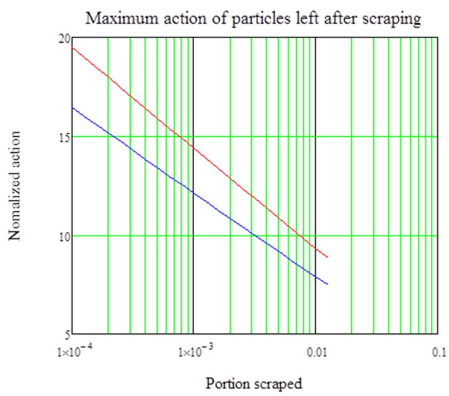

Figure 2: Variation in normalized maximum action remaining after two scraper assemblies with fraction of beam intercepted for a beam phase advance of 90^0 (blue) and 81^0 (red) between both assemblies.

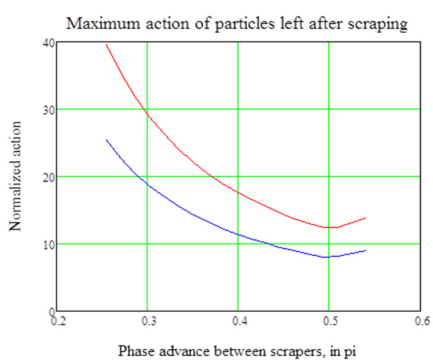

Figure 3: Variation in normalized action with beam phase advance between two scraper assemblies for beam scraping of 1% (blue) and 0.1% (red).

These analytical calculations provide a useful insight prior designing of a scraping system for the real beamline. For an instance, beam scraping of 1% at $\Delta\phi = 90^0$ results in $J_{max}=8$ while a deviation of 10% from optimal phase advance leads to an increase in J_{max} by 18%.

PI-TEST MEBT SCRAPING SYSTEM

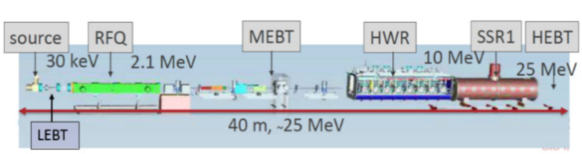

Figure 4: Layout of PI-Test facility

PI-Test (Fig. 4) consists of an ion source, a Low Energy Beam Transport (LEBT), RFQ, MEBT, two cryomodules (HWR and SSR1), and a High Energy Beam Transport (HEBT) section that carries beam to the dump. A detail description of the PI-Test is presented elsewhere [1]. The PI-Test MEBT [3] will be a 10 m long beamline composed of focusing magnets, bunching cavities, chopping system, and diagnostics. The nominal current of the beam entering the MEBT is 5 mA CW; the chopping system remove designated bunches, leaving 2 mA for injection into the cryomodules. Figure 5 shows 3σ transverse beam envelope for the passing bunches in the MEBT.

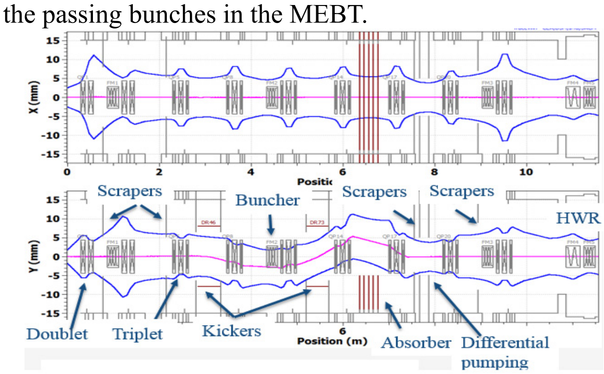

Figure 5: Horizontal (top) and vertical (bottom) 3σ beam envelope along MEBT.

The MEBT scraping system consists of four scraper assemblies. Each assembly is made of four moveable, radiation-cooled blades, designed to tolerate the deposited beam power of 100 W per assembly (~1% of beam power at the MEBT entrance, 10.5 kW). These assemblies are arranged in two pairs, and efforts are made to set the phase advance close to 90° between each pair. The first pair of assemblies are installed near the MEBT entrance and are utilized primarily to clean transverse tails of the beam coming out of the RFQ. This arrangement should prevent the beam loss at kickers which are the most sensitive elements of the MEBT. In this upstream portion of the MEBT, vacuum is of the order of $\sim 10^{-7}$ Torr, and the expected scraper outgassing does not present a problem. Correspondingly, the present scenario assumes interception of ~1% of the beam at each assembly in the first pair. On the other hand, beam coming out from the RFQ needs to be matched with the significantly larger β-functions of the MEBT that requires densely packed elements at the transition. This, in turn reduces plausible options for scraper locations. The second pair of scraper assemblies are close to the SRF section where an excessive beam scraping may result in both degradation of UH vacuum and generation of micro-particles. Thus, each of those assemblies is expected to intercepts only 0.1% of beam in nominal operating conditions. The primary objective for those scrapers is to protect the SRF cavities from beam irradiation in case of errors with beam steering or focusing as well as kicker mis-firing. Figure 6 shows horizontal and vertical beam phase advance along the MEBT. The phase advance is different in two planes and is significantly reduced by space charge forces. It is worth to mention here that the beam centroid motion relevant in a case of steering errors is characterized by the zero-current phase advance, while for the focusing errors one needs to consider space charge forces as well. Thus, choice

ISBN 978-3-95450-169-4

of the scrapers placement is a compromise between mechanical constraints and phase advances in two planes and space charge conditions. Table 1 summarizes beam phase advance between successive scrapers assemblies for the present arrangement of their location in the MEBT.

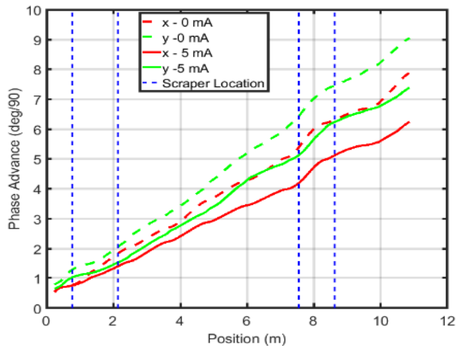

Figure 6: Beam transverse phase advance in MEBT.

Table 1: Phase Advance between Scraper Assemblies in MEBT

Beam Current		Scraper 1-2	Scraper 2-3	Scraper 3-4
0 mA	x	95.7^0	319.3^0	83.5^0
	y	69.8^0	393.1^0	92.4^0
5mA	x	58.7^0	250.5^0	83.4^0
	y	45.1^0	323.2^0	100^0

Performance of the scraper system was analysed numerically using a beamdynamics code TRACWIN [4]. A bunch with nominal initial parameters (corresponding to 5 mA beam in the LEBT and rms normalized transverse emittance of 0.21 µm) was modelled by a Gaussian distribution of one million macro particles and tracked through the MEBT. Insertions of each scrapers in the beam pipe were adjusted to intercept nominal fraction (as mentioned earlier) of the beam.

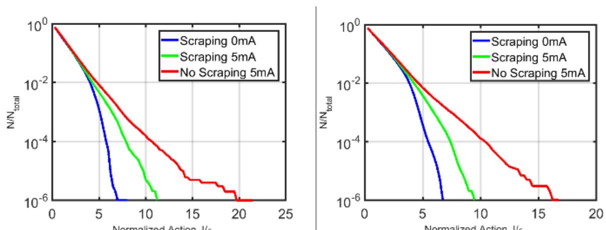

Figure 7: Particle distribution over normalized action in horizontal (left) and vertical (right) phase spaces at the end of MEBT.

The resulting particle distribution over the normalized action at the end of MEBT is shown in Fig. 7. Efficiency of the first pair of scraper assemblies in the MEBT is significantly affected by deviation of the phase advance between them from 90º especially, after accounting space charge forces. Another factor increasing the tail population is the halo formation due to non-linear space charge forces. Although the fraction of the beam scraped at the second pair of assemblies is small yet it still decreases the far tails noticeably. It is largely related to the fact that the phase advance between the pairs is far from a multiple of 90º, and therefore the second pair cuts corners of the phase space distribution (Fig. 8).

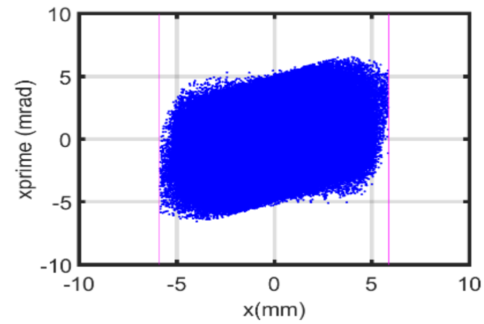

Figure 8: Particle distribution in phase space after third scraper assembly (magenta lines).

The described scraping system should protect the SRF components effectively from steering/focusing errors occurring at upstream of the scraping system. The maximum action of particles propagating to the SRF sections should still stay within the limits presented in Fig. 7, i.e. J_{max} ~10. The expected normalized rms transverse emittance in the MEBT is 0.21 µm that implies that all particles with actions above ~ 2 µm are intercepted. Taking into account that the simulated SRF acceptance is 20 µm, it leaves a large margin to ensure that SRF cavities are not irradiated at the time of problems in the front end.

CONCLUSION

Performance of the scraping system can be quantified by the maximum action of the particle distribution remaining after scraping of a given portion of the beam. For a system consisting of two scraper assemblies, this performance is optimal when the betatron phase advance between assemblies is 90º. Analytical estimations for a Gaussian particle distribution shows that scraping of 0.1%-1% of the beam can limit the maximum action of the remaining particles to 10-15 times of the rms emittance. A proposed design of the scraping system in the PI-Test MEBT should limit the maximum action to ~10 times of the input emittance and protect the SRF cavities from beam irradiation in all scenarios of steering or focusing errors occurring at upstream of the second pair of the MEBT scraper assemblies.

REFERNCES

[1] P.F. Derwent *et al.*, "PIP-II Injector Test: challenges and status", presented at LINAC'16, East Lansing, MI, USA, paper WE1A01, this conference

[2] C. Peters *et al.*, "Superconducting radio frequency cavity degradation due to errant beam", in *Proc. IPAC'15*, Busan, Korea, paper MOPHA013.

[3] A. Shemyakin *et al.*, "Design of MEBT for the Project X Injector Experiment at Fermilab", in *Proc. LINAC'12*, Tel Aviv, Israel, paper MOPB09.

[4] TraceWin code, `http://irfu.cea.fr/Sacm/logiciels/`

ISBN 978-3-95450-169-4